Landscape Ecology vol. 10 no. 1 **pp** 23-39 (1995)
SPB Academic Publishing bv, Amsterdam

A factor analysis of landscape pattern and structure metrics

K.H. Riitters[1], R.V. O'Neill[2], C.T. Hunsaker[2], J.D. Wickham[3], D.H. Yankee', S.P. Timmins[4], K.B. Jones[5] and B.L. Jackson[2]
[1]*Tennessee Valley Authority, Norris, TN 37828, USA;* [2]*Oak Ridge National Laboratory, Oak Ridge, TN 37831, USA;* [3]*Desert Research Institute, Reno, NV 89512, USA;* [4]*Analysas Corporation, Oak Ridge, TN 37830, USA;* [5]*Environmental Protection Agency, Las Vegas, NV 89193, USA*

Abstract

Fifty-five metrics of landscape pattern and structure were calculated for 85 maps of land use and land cover. A multivariate factor analysis was used to identify the common axes (or dimensions) of pattern and structure which were measured by a reduced set of ***26*** metrics. The first six factors explained about 87% of the variation in the ***26*** landscape metrics. These factors were interpreted as composite measures of average patch compaction, overall image texture, average patch shape, patch perimeter-area scaling, number of attribute classes, and large-patch density-area scaling. We suggest that these factors can be represented in a simpler way by six univariate metrics – average perimeter-area ratio, contagion, standardized patch shape, patch perimeter-area scaling, number of attribute classes, and large-patch density-area scaling.

Introduction

Over the past century, technological advances have greatly improved the standard of living in the United States. But these same advances have caused sweeping environmental changes, often unforeseen and potentially irreparable. The time has come when stewardship of the environment requires that we monitor and assess environmental changes at the national scale with a view toward the conservation and wise management of our natural resources.

Some of the most important aspects of environmental change occur at the broad spatial scale of whole landscapes. Obvious examples include deforestation, loss of wetlands, and conversion of prairies into crop and grazing systems. The potential now exists to begin landscape monitoring and assessment by combining remote satellite imagery of landcover, geographic information system (GIS) technology, and recent advances in the science of landscape ecology (Forman and Godron **1986).**

Not all environmental changes can be monitored at the landscape scale. Stream pollution or the replacement of native wildlife with introduced species may cause little or no change in landscapes that can be detected in remote imagery. To achieve complete assessments, landscape monitoring must be integrated with field studies in large programs such as the Environmental Protection Agency's Environmental Monitoring and Assessment Program (EMAP). Nevertheless, we can begin immediately to evaluate some important changes at continental scales. By integrating available technology, the effort can be rendered practical, economic, and rapid, relative to any field-based approach.

The purpose of this study was to help choose a set of landscape metrics for monitoring landscape condition in terms of land use pattern and structure. Analysis of landscape pattern and structure can consider a large number of metrics such as con-

Table 1. Descriptions of LUDA land use and land cover attribute class codes (Anderson *et al.* 1976).

LUDA class code	Anderson Level II attribute class description
11	Residential
12	Commercial, service, institutional
13	Industrial
14	Transportation
15	Industrial and commercial complex
16	Mixed urban and built-up
17	Other urban or built-up
21	Cropland and pasture
22	Orchards, vineyards, and nurseries
23	Confined feeding operations
24	Other agricultural lands
31	Herbaceous rangeland
32	Shrub-brush rangeland
33	Mixed rangeland types
41	Deciduous forest
42	Evergreen forest
43	Mixed forest types
51	Streams and canals
52	Natural lakes
53	Reservoirs
54	Bays and estuaries
61	Forested wetlands
62	Non-forested wetlands
71	Dry salt flats
72	Beach
73	Non-beach sandy area
74	Bare exposed rock
75	Strip mine, quarry, and borrow areas
76	Transitional (disturbed, little cover, not agricultural)
77	Mixed barren lands
81	Shrub-brush tundra
82	Herbaceous tundra
83	Bare ground tundra
84	Wet tundra
85	Mixed tundra
91	Perennial snowfield
92	Glacier

tagion, evenness, and fractal dimension (Turner and Gardner 1991). Ideally, there is a small set of metrics which span the important dimensions of pattern and structure, but which are not redundant (U.S. Environmental Protection Agency 1994). There were two motivating questions for this study: (1) how many independent axes of landscape pattern and structure are measured by typical landscape metrics? (2) which metrics or combinations of metrics are best suited for quantifying those axes? Starting from a large number of candidate metrics calculated for a collection of land use and land cover maps, a multivariate factor analysis was used to identify a smaller number of apparently independent axes. Such an analysis will suggest a minimum subset of individual metrics for monitoring landscapes.

Methods

USGS LUDA maps

Eighty-five maps were selected from the U.S. Geological Survey Land Use Data Analysis (LUDA) database of land use and land cover derived from high-altitude aerial photography (Fegeas *et al.* 1983). The selection was inteded to represent a rough transect of landscape patterns across physiographic regions of the United States (Hunsaker *et al.* 1994). Each LUDA map covers a 1:250000 quadrangle (– 120 km × 180 km) and, in raster format, has an extent of about 500 × 800 cells with a grain size of 200 m (Hunsaker *et al.* 1994). Each cell is classified into one of 37 possible attribute classes (Table 1).

Landscape rnetrics

New software was written to process the LUDA maps and to calculate landscape metrics. The computing formulas for the 55 landscape metrics considered in this study are given in an Appendix. The following image proacessing steps provided the information necessary to calculate the metrics for each map. First, the frequencies of different attribute classes (F_i, $i = 1 \ldots t$) and the number of attribute classes (t) were determined by counting cells. Next, the attribute adjacency matrix ($\boldsymbol{A}$) was constructed by counting the edges between cells. A_{ij} ($i,j = 1 \ldots t$) denotes the frequency of attribute class i being located adjacent to attribute class j in a cardinal direction. Because each edge was counted once, A is without regard to the ordering of the two cells that define an edge.

Individual patches were then delineated as sets of contiguous cells of the same attribute class. Only cardinal directions were considered when evaluating contiguity. Let m be the total number of patches, and S_k $(k = 1 \ldots m)$ denote the number of cells of the k-th patch. Patch area is the number of cells in a patch. Patch perimeters were determined in three different ways as: (1) the number of edges enclosing a patch (OE_k); (2) the number of cells enclosing a patch (OC_k), and; (3) the number of edges between patch k and all inclusions ('islands' of different attribute classes) contained within patch k (IE_k). The sum of IE_k and OE_k measures total perimeter edge length.

Patch centroids (CT_k) were calculated as the average row and column of the cells that are part of patch k. The rectangle which bounds patch k was defined by the maximum and minimum rows ($r_{max,k}$, $r_{min,k}$) and columns ($c_{max,k}$, $c_{min,k}$) which were occupied by cells that are part of the patch. The longest axis across patch k (LA_k) was twice the radius of the circle which contains all cells that are part of the patch (an approximate algorithm by Ritter [1990] was used). Finally, each patch was scored according to whether or not it touched the border of the map. These procedures provided the information necessary to calculate the landscape metrics shown in the Appendix.

The fractal metrics require some elaboration here. In general, fractal analyses quantify scaling relations, of the form $y - x^{\beta}$, of a landscape property y over a range of scale x. The scaling factor (β) is estimated by the slope from a double logarithmic linear regression of the form $\ln(y) = \alpha + \beta\ln(x)$. A fractal dimension is then found by transforming β (*e.g.*, Falconer 1990). Depending on the choices of y and x, and the transformation of β, the dimension may have a geometric interpretation. For example, in the classic 'coastline length' algorithm (Mandelbrot 1967), y is the apparent perimeter length of an island as measured by a divider (or ruler) of length x, and the transformation $1-\beta$ estimates a geometric dimension corresponding to perimeter complexity.

Although the mere presence of scaling does not imply a geometric dimension (Mandelbrot 1983), the general procedure can be used to quantify pattern and shapes in an image (Falconer 1990). The term 'dimension' is used in this study as a convenience. Furthermore, we considered statistical scaling as opposed to exact fractal mathematics (see discussion by Voss 1988). For this reason, it was appropriate to test the hypothesized scaling relationships; F-tests were made of the linear regression, and of the evidence for lack-of-fit to the linear model (*e.g.*, Steel and Torrie 1980).

This analysis was also concerned with overall map pattern and structure without regard to particular attribute classes. Some integrative, area-based metrics such as attribute diversity are naturally calculated for an entire map. But some other metrics are normally calculated on a per-patch or per-attribute class basis. In those cases, it was necessary to average, over patches or attribute classes, in order to obtain a comparable value for an entire map. Patches with fewer than four cells were excluded from average patch metrics because most patch-level metrics are fixed for small patch sizes (Hunsaker *et al.* 1994). When appropriate, averages over attribute classes were weighted by attribute class frequencies.

In the Appendix, each of 55 landscape metrics is described by a four-character acronym, a short verbal description, and a defining formula using the previous notation. For example, the acronyms NTYP and *NPAT* refer to the numbers of attribute classes (t) and patches (m) in the map. Some supplemental methodological information is provided where appropriate.

Factor analysis

Because many of the 55 metrics are so closely related, some of them were immediately eliminated (their definitions are retained in the Appendix for reference only). To accomplish this, all pair-wise correlation coefficients were calculated among the 55 metrics. Groups of metrics were then formed, such that all within-group correlations were larger than $+0.9$. One metric was then selected to represent each group (Table 2). One selection criterion was apparent normality, but sometimes the choice was arbitrary. This process eliminated 29 metrics,

Table 2. Groups of metrics derived from correlation, coefficients, and the representative metrics selected for factor analysis. See text for explanation of methods, and appendix for definitions of metrics.

Group number	Group members	Representative metric
1	NTYP	NTYP – Number of attribute classes
2	SIDI, SIEV, SHDI, SHEV, MCDI, MCEV, SHHO, SIHO	SHEV – Shannon evenness of attribute classes
3	KT-Q	KT-Q – Kempton-Taylor Q-statistic
4	PMAX, SHCO, SICO	SHCO – Shannon contagion
5	SUMD, TENT, TMAS, TVAR, P050, P500	SUMD – Sum of diagonal elements of adjacency matrix
6	TLAC	TLAC – Average attribute class lacunarity from the scaling of attribute density with neighborhood size
7	P005	P005 – Average proportion of area in patches larger than 5 cells
8	OEFC, OFIC, OCFC	OCFC – Perimeter-area scaling, patch perimeter complexity
9	OEFT, OIFT, OCFT	OCFT – Perimeter-area scaling, patch topology transformation, enclosing cells basis
10	ABFT, BCFT	BCFT – Patch area-bounding circle scaling
11	BETL	BETL – Patch perimeter complexity from the scaling of Euclidean distance to actual distance along large patch perimeters
12	PENT, PMAS, PVAR	PMAS – Metric of large-patch 'mass' from the scaling of patch density with neighborhood size
13	PLAC	PLAC – Average large-patch lacunarity from the scaling of patch density with neighborhood size
14	NPAT	NPAT – Number of patches
15	PSIZ	PSIZ – Average patch size or area
16	OEDG, TEDG, OPER, RGYR, LOAX	RGYR – Average patch radius of gyration
17	IEDG	IEDG – Average number of inside edges per patch
18	PA-1	PA-1 – Average patch perimeter-area ratio
19	PA-2	PA-2 – Average patch adjusted perimeter-area ratio
20	NACI, NASQ, BRRA	NASQ – Average patch normalized area, square model
21	NFTD	NFTD – Average patch topology ratio
22	PORO	PORO – Average patch ratio of number of inside edges to area
23	DSTA, ABRA	DSTA – Average patch adjusted perimeter-area ratio
24	CCRA	CCRA – Average ratio of patch area to area of the circumscribing circle
25	RGLA, LARA	RGLA – Average ratio of patch radius of gyration to long axis length
26	OPOE	OPOE – Average patch ratio of perimeter cells to perimeter edges

leaving 26 to be used in the factor analysis. Sometimes the grouping criterion retained some pairs of metrics with a correlation less than −0.9; this is important for reasons given later.

The general purpose of factor analysis is to describe the covariance structure among many variables in terms of a few underlying (but not directly observable) quantities which are called 'factors'. Among others, Morrison (1976) and McDonald (1985) provide mathematical treatments of factor analysis; Pimentel (1979) and Johnson and Wichern (1982) describe typical procedures and limitations of the approach. In this study, factor analysis proceeds by grouping the 26 metrics such that within-group correlations are large and between-group correlations are small. This step was accomplished by applying the principal components method to the correlation matrix. The number of such groups to consider further was then chosen based on (a) the eigenvalues associated with each group, (b) the plot of eigenvalue versus component number, and (c) the cumulative proportion of variance explained by

Table 3. Summary statistics for 26 selected metrics from 85 maps.

Variable	Statistic					Normally distributed?[c]
	Mean	Std Dev[a]	CV[b] (%)	Min.	Max.	
NTYP	22.541	3.030	13	17	34	No
SHEV	0.379	0.132	35	0.067	0.716	Yes
KT-Q	3.582	1.369	38	1.364	8.177	No
SHCO	0.745	0.095	13	0.488	0.951	Yes
SUMD	0.903	0.056	6	0.761	0.987	No
TLAC	0.040	0.018	45	0.001	0.081	Yes
P005	0.992	0.007	1	0.956	1.000	No
OCFC	1.242	0.049	4	1.102	1.351	Yes
OCFT	1.349	0.074	5	1.094	1.573	Yes
BCFT	1.349	0.074	5	1.094	1.573	Yes
BETL	1.358	0.079	6	1.188	1.604	Yes
PMAS	1.581	0.062	4	1.488	1.994	No
PLAC	0.008	0.004	50	0.000	0.018	Yes
NPAT	2627	2103	80	190	9061	No
PSIZ	361.5	405.1	112	48.2	2614.5	No
RGYR	3.636	1.062	29	2.207	6.963	No
IEDG	19.040	9.687	51	3.324	51.578	No
PA-1	1.400	0.148	11	1.051	1.785	Yes
PA-2	1.726	0.084	5	1.518	1.933	No
NASQ	0.532	0.037	7	0.448	0.637	Yes
NFTD	1.890	0.032	2	1.782	1.964	Yes
PORO	0.004	0.001	25	0.001	0.007	Yes
DSTA	1.342	0.027	2	1.283	1.419	Yes
CCRA	0.649	0.049	8	0.522	0.755	Yes
RGLA	0.664	0.014	2	0.627	0.698	Yes
OPOE	0.809	0.022	3	0.775	0.892	Yes

[a] Standard deviation.
[b] Coefficient of variation.
[c] Normality was tested by the W-statistic with a p-value of 0.05.

including additional groups. Each group corresponds to one axis in metric state space. To check the results of the principal components method, the maximum likelihood method was also applied, and the results were compared.

It is a common practice to interpret the axes by examining the common characteristics of metrics which form a group associated with a given axis, and the correlations ('loadings') of metrics with that axis. In an artificial example, suppose that all of the fractal metrics had high loadings on just one axis. It would be plausible to interpret the underlying factor associated with that axis as 'fractal dimension'. In general, any such interpretation is at least partly subjective because there is no rigorous procedure.

Recall that some pairs of the 26 metrics had large, but negative, correlations. **A** factor analysis should place those pairs in the same group, but give them loadings of opposite sign. The rationale for retaining these pairs was that it would help to interpret the resulting groups of metrics. It would have also been reasonable to exclude one member of each of these pairs from further analysis. The choice of metrics to consider in a factor analysis will affect the results, but whether or not some highly-correlated pairs are retained will make little difference at the interpretation stage. The most interesting feature of the analysis will be how pairs of metrics with medium and small correlations will be grouped.

To help elucidate the underlying factors, it is also a common practice to 'rotate' the selected axes. Both orthogonal and oblique rotations are possible. **An** orthogonal rotation, such as the varimax rotation, preserves the relative orientation between axes, but an oblique rotation does not. In this study, both orthogonal and oblique rotations were performed; however, all of the results are presented in terms of the orthogonal varimax rotation.

Representative maps were then chosen to illustrate the results of the factor analysis. These choices were based on the factor scores for each map. For a given map and factor, a factor score is calculated as the weighted sum of all 26 metrics, where the weights are the loadings for that factor. In geometric terms, the scores are the relative positions of different maps along the axis corresponding to a given factor.

Results and discussion

Simple summary statistics for 26 metrics are shown in Table **3.** The number of attribute classes per map varied from 17 to **34,** the number of patches from 190 to 9061, and the average patch size from 48 to 2615 cells. The patch statistics cited here are for patches larger than **3** cells. When all patches are considered (this case is not shown in Table **3),** their total number varied from 247 to 16610, and their average sizes were smaller.

Table 4. Pearson correlation coefficients (n = 85) among the metrics chosen for factor analysis. Absolute values > **0.27** are significar at $p = 0.01$ and are underlined.

Metric number/ acronym		1	2	3	4	5	6	7	8	9	10	11	12	13	14	15	16	17	18	19	20	21	22	23	24	25	26
1	NTYP																										
2	SHEV	0.24																									
3	KT-Q		-0.27	--																							
4	SHCO	-0.16	-0.97	0.29																							
5	SUMD	-0.00	-0.73	0.26	0.86	--																					
6	TLAC	0.12	0.86	-0.30	-0.82	-0.53																					
7	P005	-0.19	-0.57	-0.02	0.68	0.78	-0.35	--																			
a	OCFC	-0.14	0.32	-0.23	0.45	-0.67	0.17	-0.39	--																		
9	OCFT	0.12	-0.33	0.22	0.46	0.67	-0.19	0.40	-1.00	--																	
10	BCFT	0.00	0.33	-0.30	-0.24	0.00	0.38	0.24	-0.36	0.37	--																
11	EETL	-0.05	0.25	-0.05	-0.40	-0.67	0.15	-0.54	0.72	-0.73	-0.42	--															
12	PMAS	0.08	-0.21	0.15	0.28	0.36	-0.18	0.22	-0.28	0.28	-0.03	0.03	--														
13	PLAC	0.10	0.14	-0.01	0.02	0.35	0.21	0.39	-0.43	0.43	0.51	-0.66	0.18	--													
14	NPAT	0.00	0.64	-0.22	-0.78	-0.95	0.48	-0.81	0.57	-0.57	-0.08	0.68	-0.34	-0.44	--												
15	PSIZ	-0.23	-0.49	-0.02	0.56	0.63	-0.41	0.52	-0.65	0.68	0.40	-0.59	0.34	0.31	-0.58	--											
16	RGYR	-0.24	-0.14	-0.19	0.27	0.51	-0.04	0.60	-0.48	0.50	0.63	-0.71	0.19	0.68	-0.59	0.74	--										
17	IEDG	-0.35	-0.68	-0.03	0.75	0.74	-0.53	0.67	-0.46	0.48	0.19	-0.52	0.20	0.26	-0.74	0.74	0.61	--									
18	PA-1	0.22	0.04	0.18	-0.18	-0.45	-0.12	-0.65	0.51	-0.52	-0.72	0.65	-0.06	-0.65	0.50	-0.58	-0.86	-0.52	--								
19	PA-2	-0.10	0.38	-0.39	-0.40	-0.40	0.26	-0.08	0.57	-0.56	0.28	0.17	-0.21	0.08	0.19	-0.22	0.20	-0.15	-0.02	--							
20	NASQ	-0.02	-0.32	0.33	0.35	0.39	-0.21	0.19	-0.47	0.46	-0.22	-0.20	0.20	0.08	-0.24	0.23	-0.02	0.20	-0.18	-0.91	--						
21	NFTD	-0.14	0.15	-0.17	-0.06	0.16	0.27	0.40	-0.33	0.33	0.62	-0.36	0.05	0.43	-0.14	-0.36	0.46	0.23	-0.73	-0.20	0.33	--					
22	PORO	0.33	0.41	0.09	-0.45	-0.48	0.27	-0.42	0.26	-0.27	0.00	0.28	-0.24	-0.13	0.39	-0.53	-0.38	-0.52	0.30	0.15	-0.15	-0.19	--				
23	OSTA	-0.20	-0.16	-0.05	0.30	0.56	0.02	0.64	-0.65	0.66	0.58	-0.67	0.14	0.61	-0.54	0.63	0.79	0.56	-0.95	-0.29	0.47	0.73	-0.33	--			
24	CCRA	0.09	-0.12	0.30	0.07	-0.04	-0.14	-0.21	-0.06	0.06	-0.42	0.27	0.14	-0.30	0.19	-0.08	-0.47	-0.16	0.31	-0.79	-0.79	0.16	0.06	-0.04			
25	RGLA	0.17	-0.12	0.34	0.01	-0.22	-0.22	-0.47	0.22	-0.24	-0.74	0.52	0.07	-0.54	0.34	-0.36	-0.76	-0.36	0.75	-0.56	-0.48	-0.37	0.20	-0.52	0.84		
26	OPOE	-0.05	-0.43	0.33	0.47	0.47	-0.34	0.24	-0.36	-0.36	-0.35	-0.23	0.15	0.09	-0.38	0.20	0.10	0.28	-0.16	-0.66	0.82	-0.07	-0.16	0.40	0.49	0.36	

Table 5. Results of principal components factor analysis and varimax rotation of the first six factors.

	Component number						
	1	2	3	4	5	6	
	Eigenvalues and cumulative proportion of variance explained by principal components analysis						
Eigenvalue	9.863	5.551	3.102	1.886	1.098	0.984	
Cum. variance	37.9	59.3	71.2	78.5	82.7	86.5	
	Factor pattern after varimax rotation						**Communalitv**
DSTA	0.883	0.201	0.271	0.217	-0.161	0.005	0.97
PLAC	0.814	0.008	-0.097	0.015	0.253	0.121	0.75
RGYR	0.806	0.303	-0.255	0.196	-0.160	0.104	0.88
NFTD	0.706	-0.216	0.252	0.176	-0.316	0.117	0.75
BCFT	0.681	-0.292	-0.348	0.408	-0.141	0.011	0.86
BETL	-0.673	-0.385	0.032	-0.401	-0.191	0.221	0.85
RGLA	-0.697	-0.071	0.655	-0.114	0.134	0.070	0.96
PA-1	-0.935	-0.135	0.019	-0.143	0.201	0.017	0.95
SHCO	0.035	0.955	0.183	0.128	0.013	0.062	0.97
SUMD	0.402	0.815	0.164	0.179	0.182	0.140	0.94
IEDG	0.360	0.752	-0.015	0.220	-0.278	0.052	0.82
P005	0.595	0.658	-0.009	-0.097	-0.083	0.100	0.81
PORO	-0.171	-0.467	-0.027	-0.150	0.403	-0.324	0.54
NPAT	-0.483	-0.790	-0.007	-0.054	-0.223	-0.125	0.93
TLAC	0.296	-0.832	-0.107	-0.104	0.006	-0.006	0.80
SHEV	0.133	-0.933	-0.185	-0.100	0.075	-0.017	0.94
NASQ	0.182	0.170	0.958	0.101	0.027	0.033	0.99
CCRA	-0.287	-0.114	0.903	0.031	-0.021	0.128	0.93
OPOE	0.155	0.410	0.739	-0.110	0.130	-0.086	0.77
PA-2	0.046	-0.185	-0.883	-0.354	-0.112	-0.055	0.96
OCFT	0.456	0.313	0.257	0.731	0.205	0.063	0.95
PSIZ	0.401	0.507	0.005	0.569	-0.254	0.237	0.86
OCFC	-0.452	-0.304	-0.266	-0.720	-0.229	-0.062	0.94
NTYP	-0.064	-0.218	-0.006	0.131	0.845	0.100	0.79
KT-Q	-0.140	0.229	0.317	0.051	0.684	0.051	0.65
PMAS	0.066	0.199	0.106	0.068	0.120	0.921	0.92
							Sum 22.48
	Variance explained by each factor after rotation						
	6.626	6.247	4.180	2.178	2.050	1.204	

The correlation coefficients of all pairs among 26 metrics are shown in Table 4. The preliminary screening of metrics did not eliminate all statistically significant correlations; roughly one-half of the coefficients exceed the critical value for statistical significance ($\pm$ 0.27, p = 0.01). Some metrics (*e.g.*, NTYP and KT-Q) have relatively fewer significant correlations with other metrics, while others (*e.g.*, OCFT and OCFC) have relatively more. The number of significant correlations in Table **4** suggests that a multivariate approach to data reduction will be productive.

After factoring the correlation matrix by the principal components method, the first six factors together explained about 87% of the variation in the 26 landscape metrics (Table 5). A rule-of-thumb for retaining factors is that the associated eigenvalue be greater than one. The first five factors met this criterion, and the sixth was retained because it appeared to be uniquely and strongly associated with just one of the landscape metrics (PMAS). The communality estimate for each metric (Table 5) is the squared multiple correlation for predicting that metric from the six factors; those metrics with low communality are associated with relatively more of the unexplained variance in the correlation matrix.

The loadings of each metric on each of the first six factors after orthogonal rotation are shown by the factor pattern in Table 5. For example, the fourth factor has relatively high loadings for the metrics OCFT (0.731) and OCFC (−0.720). This means that in the rotated metric state space, both OCFT and OCFC lie near the fourth axis. Furthermore, because the signs differ, those metrics lie near opposite ends of the fourth axis; either metric alone would characterize the fourth axis with almost equal utility because their absolute values are approximately equal. This is an example of how a metric pair with high negative correlation is treated by a factor analysis.

The dimensions were interpreted by examining the factor pattern in Table 5. The first axis was termed *averagepatch compaction* because it is most correlated with measures of average patch compaction (PA-1, DSTA, RGYR) and large-patch texture (PLAC). The second axis is most correlated with measures of whole-map attribute and edge-type frequencies (SHCO, SHEV, TLAC, SUMD); overall this axis appears to measure *image texture.* The third axis *(averagepatch shape)* is most correlated with those average patch metrics which employ standardization to an assumed patch shape (NASQ, CCRA, PA-2). The fourth axis is associated with the perimeter-area fractal measures (OCFT and OCFC) leading to the name *patch perimeter-area scaling.* The fifth axis is most correlated with the *number of attribute classes* (NTYP) which is a convenient label. The sixth axis is correlated only with PMAS, a measure of *large-patch density-area scaling.*

The oblique rotation did not change the orientation of any axis by more than 10" (these results are not shown), and as a result, the interpretations of factors did not change. The maximum likelihood method of factoring did change the order of the first five factors, but not the relative loadings of metrics on a given factor (these results are not shown), and the sixth axis was not retained. The change of order implied a difference only in the relative importance of the hypothesized factors. The loss of the sixth axis was traced to a single (outlier) map which was essentially one large patch; the principal components method placed more importance on this outlier map than did the maximum likelihood method.

Eight maps which represent extremes along one or more of the first four axes are shown in Figure 1 (Table 6 gives the associated factor scores). The figure provides a visual impression of the types of pattern and structure corresponding to the first four factors. For example, the maps 'Sterling' and 'Wilmington' (Case A in Figure 1) are at opposite ends of the first axis (their factor scores have opposite signs in Table 6) and thus show differences in average patch compaction. Cases B, C, and D illustrate differences in image texture, average patch shape, and patch perimeter-area scaling, respectively. The factor scores (Table **6)** can be used to select additional pairs from these eight maps for other visual contrasts; some maps illustrate extremes of more than one axis. For example, the map 'Wilmington' illustrates extremes of image texture as well as average patch compaction.

It is easier to visualize the ordination of each map

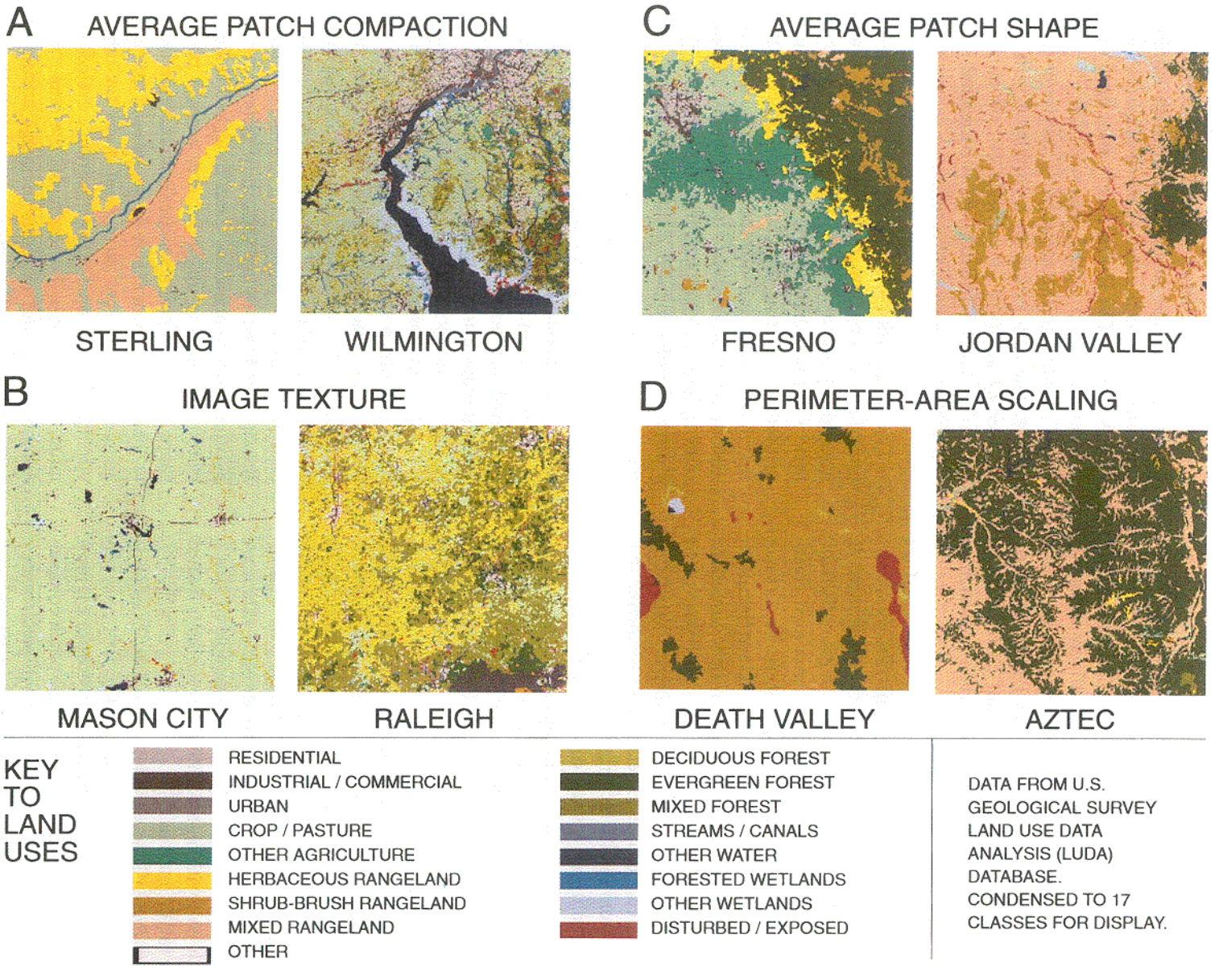

Fig. 1. A comparison of LUDA maps which had relatively high and low factor scores for the first four axes from the factor analysis (see Table 6). Map pairs labeled A through D are contrasts of average patch compaction (factor 1), image texture (factor 2), average patch shape (factor 3), and patch perimeter-area scaling (factor 4), respectively.

Table 6. First four factor scores for eight representative LUDA maps.

LUDA map	Factor 1	2	3	4
	Factor score			
Sterling	2.3	0.3	2.3	−0.7
Wilmington	−2.2	−2.2	−1.0	**1.8**
Mason City	−2.9	2.2	0.0	−1.0
Raleigh	−0.3	−2.1	1.9	0.6
Fresno	**1.0**	−0.7	2.2	−0.8
Jordan Valley	−0.4	1.0	−2.4	0.3
Death Valley	1.0	1.3	0.5	3.9
Aztec	0.5	***0.6***	−0.9	−2.1

in the first four dimensions by using a star symbol for each map (Figure 2). The first four factor scores are represented by a four-armed star; each arm represents a different factor, and the arm length is proportional to the factor score. Thus, 'flattop' symbols correspond to small scores for factor 2, implying 'fine' texture (*e.g.*, 'Raleigh' in Figure 1). Two maps with similar pattern and structure will have similar symbols, meaning that their factor scores place them closer together in four-space.

By interpreting the star symbols according to the geographic location of the corresponding USGS quadrangle (as shown in Figure 2), larger spatial patterns of landscape pattern and structure condition can be hypothesized. For example, the fine texture maps occur most often in the southeast U.S., whereas the western maps more commonly had coarse texture. This supports a hypothesis that the southeast region has a relatively high degree of fragmentation (equivalently, low contagion) of land use in comparison to the western region. In another example, many of the midwestern maps are characterized by coarse texture, and linear patches with complicated perimeters. These patterns are consistent with a low fragmentation of predominantly agricultural land uses, and the interspersion of linear transportation corridors and meandering rivers among otherwise homogeneous landscapes. These geographic interpretations of whole-map metrics would probably be more robust if the maps had been bounded by natural region boundaries (for example, by ecoregion or soil type boundaries) instead of by latitude and longitude. Such interpretations are also contingent on the data and procedures used to make the maps – other maps of these same areas may or may not display the same geographic trends.

To simplify the mental model and to facilitate comparisons among different sets of maps, it is worth considering a choice of single metrics which could be used as surrogates of the first six factors. The use of six metrics, instead of 55 or even ***26*** metrics, is a simplification which ignores some potential gain of precision, but at the same time, it avoids both the difficulty of interpreting linear combinations of many metrics, and the need to calculate them all for each map. Again, the choices are somewhat arbitrary, but a simple rule is to choose the single metrics with the highest loading on each factor (the criteria could include normality, relative coefficient of variation, or other considerations). This is reasonable when, as in the present case, these loadings are very high for at least one metric per factor, and that metric has a high loading for only that factor. In Table 5, the six metrics with the highest correlations with each of the six factors are PA-I (−0.935), SHCO (0.955), NASQ (0.958), OCFT (0.731), NTYP (0.845), and **PMAS** (0.921). Except for OCFT, the other five of the six loadings for each metric are relatively small, indicating that those metrics are uniquely correlated with just one factor.

Conclusion

Through a multivariate factor analysis, the 55 metrics of landscape pattern and structure that were calculated for 85 maps were found to measure six common and orthogonal factors or dimensions which were called 'average patch compaction,' 'image texture,' 'average patch shape,' 'patch perimeter-area scaling,' 'the number of attribute classes,' and 'large patch density-area scaling.'. The importance of the sixth factor was questioned because it served only to identify a single map, apparently an outlier,

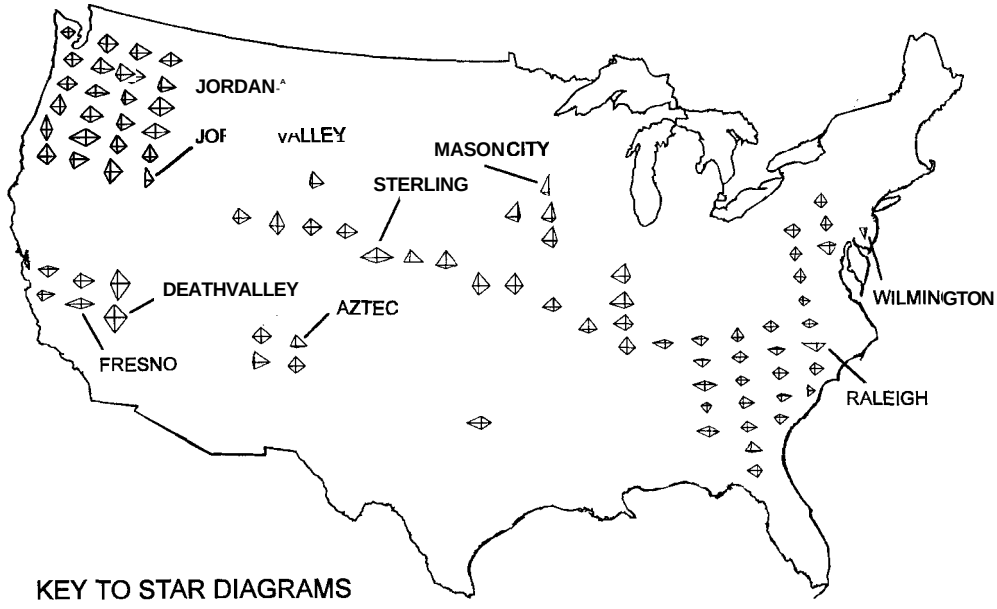

FACTOR	MEANING OF: MINIMUM VALUE	MAXIMUM VALUE
A	COMPACT PATCHES	NOT COMPACT PATCHES
B	FINE IMAGE TEXTURE	COARSE IMAGE TEXTURE
C	LINEAR PATCHES	PLANAR PATCHES
D	COMPLICATED PERIMETERS	SIMPLE PERIMETERS

Fig. 2. The first four factor scores for each **LUDA** map are represented by a 'star' symbol. Each arm of the star represents a different factor, and the length of an arm is proportional to the factor score for that map. The maps which are shown in Figure 1 are labeled here for comparison. See text for additional explanation.

and because a statistical technique which is more resistant to outliers did not identify this sixth factor as important. The factor pattern suggested that the first five factors may be adequately represented by five univariate metrics: average patch perimeter-area ratio (PA-1), Shannon contagion (SHCO), average patch area normalized to the area of a square with the same perimeter (NASQ), patch perimeter-area scaling (OCFT), and the number of attribute classes (NTYP).

It is probable that other dimensions could be identified by considering maps of different scales (number of attribute classes, map grain size, map extent), or by considering additional metrics which are not strongly correlated with those studied here, or by considering a different set of maps. These possibilities emphasize the role of factor analysis as a descriptive tool. It would be incorrect to infer that a single factor analysis has identified all important dimensions of landscape pattern that could be found. But, if the same sets of landscape metrics are found through experience in many situations, then our confidence in using these results will be greater.

There are other reasons for further research. One question which a factor analysis cannot answer is the relevance of any particular metric to a land use analyst. For example, while a factor analysis can show which metrics appear to measure image texture or contagion, it cannot indicate whether or not contagion is worth measuring at all. The answer to

that question depends upon the goal of the analysis. Another important but unanswered question for landscape monitoring is the relative sensitivity of similar metrics to real land use changes over time. For example, given that a change in average patch shape has occurred, it would be nice to know which of the several metrics of patch shape are most likely to change as a result. Finally, the statistical and sampling details of most landscape metrics need to be better-known if the metrics are to be used effectively for environmental monitoring.

Acknowledgements

The research described in this article has been funded in part by the United States environmental Protection Agency through Interagency Agreement DW64935962-01-0 with the Tennessee Valley Authority, in cooperation with the Southern Appalachian Man and the Biosphere Program, through Interagency Agreement DW89934921-01-0 with the U.S. Department of Energy, and through Cooperative Agreement CR-819549-01-5 with the Desert Research Institute.

References

Anderson, J.R., Hardy, E.E., Roach, J.T. and Witmer, R.E. 1976. A land use and land cover classification system for use with remote sensor data. Geological Survey Professional Paper 964, U.S. Geological Survey, Washington DC.

Baker, W.L. and Cai, Y. 1992. The r.le programs for multiscale analysis of landscape structure using the GRASS geographical information system. Landscape Ecology 7: 291–302.

Falconer, K. 1990. Fractal Geometry. Mathematical Foundations and Applications. John Wiley and Sons, Chichester U.K.

Fegeas, R.G., Claire, R.W., Guptil, S.C., Anderson, K.E. and Hallam, C.A. 1983. Land use and land cover digital data. Geological Survey Circular 895-E, U.S. Geological Survey, Washington DC.

Forman, R.T.T. and Godron, M. 1986. Landscape Ecology. John Wiley and Sons, New York NY.

Gonzalez, R.C. and Woods, R.E. 1992. Digital Image Processing. Addison-Wesley, Reading MA.

Hunsaker, C.T., O'Neill, R.V., Jackson, B.L., Timmins, S.P., Levine, D.A. and Norton, D.J. 1994. Sampling to characterize landscape pattern. Landscape Ecology, in press.

Johnson, R.A. and Wichern, D.W. 1982. Applied Multivariate Statistical Analysis. Prentice-Hall, Inc., Englewood Cliffs NJ.

Li, H. and Reynolds, J.F. 1993. A new contagion index to quantify spatial patterns of landscapes. Landscape Ecology 8: 155–162.

Lovejoy, S. 1982. Area-perimeter relation for rain and cloud areas. Science 216: 185–187.

Magurran, A.E. 1988. Ecological diversity and its measurement. Princeton University Press, Princeton NJ.

Mandelbrot, B.B. 1967. How long is the coast of Britain? Statistical self-similarity and fractional dimension. Science 155: 636–638.

Mandelbrot, B.B. 1983. The Fractal Geometry of Nature. W.H. Freeman and Company, New York NY.

McDonald, R.P. 1985. Factor Analysis and Related Methods. Lawrence Eribaum Associates, Hillsdale NJ.

Milne, B.T. 1991. Lessons from applying fractal models to landscape patterns. pp. 199–235 *in* Turner, M.G. and Gardner, R.H. (editors), Quantitative Methods in Landscape Ecology, Springer-Verlag, New York NY.

Morrison, D.F. 1976. Multivariate Statistical Methods. Second Edition. McGraw-Hill Inc., New York NY.

Musick, H.B. and Grover, H.D. 1991. Image textural measures as indices of landscape pattern. pp. 77–103 *in* Turner, M.G. and Gardner, R.H. (editors). Quantitative Methods in Landscape Ecology, Springer-Verlag, New York NY.

O'Neill, R.V., Krummel, J.R., Gardner, R.H., Sugihara, G., Jackson, B., DeAngelis, D.L., Milne, B.T., Turner, M.G., Zygmunt, B., Christensen, S.W., Dale, V.H. and R.L. Graham. 1988. Indices of landscape pattern. Landscape Ecology 1: 153–162.

Pickover, C.A. 1990. Computers, Pattern, Chaos and Beauty, Graphics from an Unseen World. St. Martin's Press, New York NY.

Pimentel, R.A. 1979. Morphometrics, The Multivariate Analysis of Biological Data. Kendall/Hunt Publishing Co., Dubuque IA.

Plotnick, R.E., Gardner, R.H. and O'Neill, R.V. 1993. Lacunarity indices as measures of landscape texture. Landscape Ecology 8: 201–211.

Ritter, J. 1990. An efficient bounding sphere. pp. 301–303 *in* Glassner, A.S. (editor), Graphics Gems, Academic Press, San Diego CA.

Steel, R.G.D. and Torrie, J.H. 1980. Principles and Procedures of Statistics, A Biometrical Approach. Second Edition. McGraw-Hill Book Company, New York NY.

Turner, **M.G.** and Gardner, R.H. (editors). 1991. Quantitative Methods in Landscape Ecology, Springer-Verlag, New York NY.

United States Environmental Protection Agency. 1994. Landscape monitoring and assessment research plan. U.S. EPA 620/R-94-009. Office of Research and Development, Washington DC 20460.

Voss, R.F. 1988. Fractals in nature: From characterization to simulation. pp. 21–70 *in* Peitgen, H.-O., and Saupe, D. (editors), The Science of Fractal Images, Springer-Verlag, New York NY.

Weins, **J.A.** and Milne, B.T. 1989. Scaling of 'landscapes' in landscape ecology, or, landscape ecology from a beetle's perspective. Landscape Ecology **3:** 87–96.

Appendix: Computing formulas for landscape metrics

Note: Useful review articles include Magurran (1988) for measures of attribute diversity and evenness, Milne (1991) for the application of many fractal measures to landscape analysis, and Musick and Grover (1991) for a discussion of image textural measures. Gonzales and Woods (1992) provide an introduction and overview of many metrics from the perspective of classical image analysis. Most of the metrics in this Appendix are from peer-reviewed literature, citations are intended to show where computing formulas are readily accessible. Original citations are given for only the relatively uncommon or new metrics. For yet other metrics, we can only provide a short description and manuscript title in this space.

PMAX: The maximum attribute class proportion.

where $$PMAX = sup\{p_i\}$$

$$p_i = \frac{F_i}{\Sigma_{i=1}^{t} F_i}$$

KT-Q: Kempton-Taylor Q statistic, the inter-quartile slope of the cumulative attribute abundance curve (*e.g.*, Magurran 1988).

$$KT\text{-}Q = \frac{\frac{n_{R1}}{2} + \frac{n_{R2}}{2} + \Sigma_{R=R1+1}^{R2-1} n_R}{\ln(\frac{R2}{R1})}$$

where n_R = the number of attribute classes with abundance R, $R1$ and $R2$ are the 25th and 75th quartiles (see below),

$n_{R1} = F_i$ in the attribute class where $R1$ falls,

$n_{R2} = F_i$ in the attribute class where $R2$ falls.

The quartiles are chosen such that

$$\Sigma_{R=1}^{R1-1} n_R < \frac{t}{4} \leq \Sigma_{R=1}^{R1} n_R$$

and

$$\Sigma_{R=1}^{R2-1} n_R < \frac{3t}{4} \leq \Sigma_{R=1}^{R2} n_R$$

SIDI: Simpson diversity of attribute classes.

$$SIDI = 1 - \Sigma_{i=1}^{t} p_i^2$$

SIEV: Simpson evenness of attribute classes. claljf

$$SIEV = \frac{SIDI}{1 - \frac{1}{t}}$$

SHDI: Shannon diversity of attribute classes.

$$SHDI = -\Sigma_{i=1}^{t} (p_i \ln(P_i))$$

where In denotes the base of the natural logarithms.

SHEV: Shannon evenness of attribute classes.

$$SHEV = \frac{SHDI}{\ln(t)}$$

MCDI: McIntosh diversity of attribute classes (Magurran 1988).

$$MCDI = \frac{N - \sqrt{\Sigma_{i=1}^{t} F_i^2}}{N - \sqrt{N}}$$

where

$$N = \Sigma_{i=1}^{t} F_i$$

MCEV: McIntosh evenness of attribute classes.

$$MCEV = \frac{N - \sqrt{\Sigma_{i=1}^{t} F_i^2}}{N - \frac{N}{\sqrt{t}}}$$

SUMD: Sum of diagonal elements of the adjacency matrix, **A**.[1]

[1] Wickham, J.D. and Riitters, K.H., Sensitivity of landscape metrics to pixel size. Unpublished manuscript.

$$SUMD = \Sigma_{i=1}^{t} v_{ii}$$

where

$$v_{ij} = \frac{A_{ij}}{\Sigma_{i=1}^{t} \Sigma_{j=1}^{t} A_{ij}}$$

SIHO: Simpson homogeneity of adjacency matrix[2].

$$SIHO = 1 - \Sigma_{i=1}^{t} \Sigma_{j=1}^{t} v_{ij}^2$$

The complement of SIHO is sometimes called the angular second moment (*e.g.*, Musick and Grover 1991).

SICO: Simpson contagion[2].

$$SICO = 1 - \frac{SIHO}{1 - \frac{1}{t^2}}$$

SICO is the complement of the Simpson evenness of the adjacency matrix.

SHHO: Shannon homogeneity of the adjacency matrix.

$$SHHO = - \Sigma_{i=1}^{t} \Sigma_{j=1}^{t} v_{ij} \ln(v_{ij}))$$

SHCO: Shannon contagion (O'Neill et al. 1988; Li and Reynolds 1993).

$$SHCO = I - \frac{SHHO}{2 \ln(t)}$$

SHCO is the complement of the Shannon evenness of the adjacency matrix.

PSIZ: Average patch area (number of cells).

$$PSIZ = \frac{1}{m} \Sigma_{k=1}^{m} S,$$

OEDG: Average number of edges enclosing a patch ('outside edges').

$$OEDG = \frac{1}{m} \Sigma_{k=1}^{m} OE,$$

OPER: Average number of pixels enclosing a patch ('outside pixels').

$$OPER = \frac{1}{m} \Sigma_{k=1}^{m} OC_k$$

IEDG: Average number of edges between a patch and its inclusions ('inside edges').

$$IEDG = \frac{1}{m} \Sigma_{k=1}^{m} IE_k$$

TEDG: Average total number of perimeter edges (or 'perimeter length') per patch.

$$TEDG = IEDG + OEDG$$

RGYR: Average radius of gyration (Pickover 1990).

$$RGYR = \frac{1}{m} \Sigma_{k=1}^{m} RG_k$$

where, given patch centroid CT_k, the radius of gyration (RG) of patch k is:

$$RG_k = \sqrt{\Sigma_{b=1}^{S_k} d_b^2}$$

and d_b is the distance from cell b to CT_k.

LOAX: Average length of long axis.

$$LOAX = \frac{1}{m} \Sigma_{k=1}^{m} LA_k$$

PA-1: Average perimeter-area ratio.

$$PA-1 = \frac{1}{m} \Sigma_{k=1}^{m} \frac{OE_k}{S_k}$$

PA-2: Average adjusted perimeter-area ratio (Baker and Cai 1992).

$$PA-2 = \frac{1}{m} \Sigma_{k=1}^{m} 0.282 \frac{OE_k}{\sqrt{S_k}}$$

NASQ: Average normalized area, square model.

$$NASQ = \frac{1}{m} \Sigma_{k=1}^{m} 16 \frac{S_k}{OE_k^2}$$

NASQ has a value of zero for linear patches and one for square patches, and it is sensitive to patch size.

NACI: Average normalized area, circular model.

$$NACI = \frac{1}{m} \Sigma_{k=1}^{m} 4 \pi \frac{S_k}{OE_k^2}$$

BRRA: Average bounding rectangle ratio.

---

[2] Riitters, K.H., O'Neill, R.V., Wickham, J.D. and Jones, K.B. A note on contagion metrics for landscape analysis. Unpublished manuscript.

$$\text{BRRA} = \frac{1}{m} \Sigma_{k=1}^{m} \frac{S_k}{X_k}$$

where

$$X_k = (r_{\max_k} - r_{\min_k}) \times (C_{\max_k} - C_{\min_k})$$

NFTD: Average topology ratio[3].

$$NFTD = \frac{1}{m} \Sigma_{k=1}^{m} 2 - \frac{(OC_k - OC_{\min_k})}{(OC_{\max_k} - OC_{\min_k})}$$

where

$$OC_{\min_k} = 4 \sqrt{S_k}$$

$$OC_{\max_k} = (2\ S_k) + 2$$

PORO: Average ratio of number of inside edges to area.

$$\text{PORO} = \frac{1}{m} \Sigma_{k=1}^{m} \frac{IE_k}{S_k}$$

DSTA: Average adjusted area-perimeter ratio (Gardner's D-statistic).

$$DSTA = \frac{1}{m} \Sigma_{k=1}^{m} \frac{\ln(4\ S_k)}{\ln(OE_k)}$$

ABRA: Average ratio of area to largest bounding rectangle dimension.

$$ABRA = \frac{1}{m} \Sigma_{k=1}^{m} \frac{\ln(S_k)}{Y_k}$$

where

$$Y_k = sup(r_{\max_k} - r_{\min_k}, c_{\max_k} - c_{\min_k})$$

CCRA: Average ratio of area to the area of a circumscribing circle (Baker and Cai 1992).

$$CCRA = \frac{1}{m} \Sigma_{k=1}^{m} \frac{S_k}{\pi (\frac{LA_k}{2})^2}$$

OPOE: Average ratio of perimeter cells to perimeter edges.

$$\text{OPOE} = \frac{1}{m} \Sigma_{k=1}^{m} \frac{OC_k}{OE_k}$$

RGLA: Average ratio of radius of gyration to long axis length.

$$\text{RGLA} = \frac{1}{m} \Sigma_{k=1}^{m} \frac{2\ RG_k}{LA_k}$$

LARA: Average ratio of area to long axis length.

$$\text{LARA} = \frac{1}{\text{m}} \Sigma_{k=1}^{m} \overline{ln(LA_k)}$$

P005: Weighted average proportion of cells contained in patches with area > 5 cells (Jackson's contagion5 statistic)[4].

$$P005 = \Sigma_{i=1}^{t} w_i \frac{\Sigma_{g=1}^{m_i} S_g^*}{\Sigma_{g=1}^{m_i} S_g}$$

where g subscripts patches, m_i is the total number of patches of type i,

$$S_g^* = 0 \text{ if } S_g < 6$$
$$= S_g \text{ otherwise}$$

and

$$w_i = \frac{F_i}{\Sigma_{i=1}^{t} F_i}$$

P050: Weighted average proportion of cells contained in patches with area > 50 cells.

$$P050 = \Sigma_{i=1}^{t} w_i \frac{\Sigma_{g=1}^{m_i} S_g^*}{\Sigma_{g=1}^{m_i} S_g}$$

where

$$S_g^* = 0 \text{ if } S_g < 51$$
$$= S_g \text{ otherwise}$$

P500: Weighted average proportion of cells contained in patches with area > 500 cells.

$$P500 = \Sigma_{i=1}^{t} w_i \frac{\Sigma_{g=1}^{m_i} S_g^*}{\Sigma_{g=1}^{m_i} S_g}$$

where

$$S_g^* = 0 \text{ if } S_g < 501$$
$$= S_g \text{ otherwise}$$

---

[3] Riitters, K.H. and O'Neill, R.V., Interpreting dimensions from perimeter-area scaling. Unpublished manuscript.

[4] O'Neill, R.V., Hunsaker, C.T., Timmins, S.P., Jackson, B.L., Riitters, K.H. and Wickham, **J.D.** Quantifying landscape status and trends at the regional scale. Unpublished manuscript.

OEFC: Fractal estimator of patch perimeter complexity from perimeter-area scaling, enclosing edges basis (Lovejoy 1982).

$$OEFC = 2\beta_1$$

where β_1 is the estimated slope from the regression of $\ln(OE_k)$ on $\ln(S_k)$ for all patches with $S_k > 3$ that do not touch the border of the map.

OEFT: Fractal estimator of patch topology from perimeter-area scaling, enclosing edges basis[3].

$$OEFT = \frac{1}{\beta_1}$$

OCFC: Fractal estimator of patch perimeter complexity from perimeter-area scaling, enclosing cells basis.

$$OCFC = 2\beta_2$$

where β_2 is the estimated slope from the regression of $\ln(OC_k$ on $\ln(S_k)$ for all patches with $S_k > 3$ that do not touch the border of the map.

OCFT: Fractal estimator of patch topology from perimeter-area scaling, enclosing cells basis.

$$OCFT = \frac{1}{\beta_2}$$

OIFC: Fractal estimator of patch perimeter complexity from perimeter-area scaling, all edges basis.

$$OIFC = 2\beta_3$$

where β_3 is the estimated slope from the regression of $\ln(OE_k + IE,)$ on $\ln(S_k)$ for all patches with $S_k > 3$ that do not touch the border of the map.

OIFT: Fractal estimator of patch topology from perimeter-area scaling, all edges basis.

$$OIFT = \frac{1}{\beta_3}$$

ABFT: Fractal estimator of patch topology from area-bounding rectangle scaling.

$$ABFT = \beta_4$$

where β_4 is the estimated slope from the regression of $\ln(S_k)$ on

$$\ln(\max(r_{\max_k} - r_{\min_k}, c_{\max_k} - c_{\min_k}))$$

for all patches with $S_k > 3$ that do not touch the border of the map.

BCFT: Fractal estimator of patch topology from area-bounding circle scaling.

$$BCFT = \beta_5$$

where β_5 is the estimated slope from the regression of $\ln(S_k)$ on $\ln(LA_k/2)$ for all patches with $S_k > 3$ that do not touch the border of the map.

BETL: Fractal estimator of perimeter complexity from the scaling of Euclidean distance to actual distance along patch perimeters (Weins and Milne 1989).

$$BETL = \frac{1}{u} \sum_{v=1}^{u} \frac{1}{\beta_{6v}}$$

where β_{6v} is the estimated slope from the v-th regression (v = 1 ... u patches with area > 400) of ln(Euclidean perimeter distance) on ln(actual) perimeter distance). Riitters[5] describes the procedures as follows. For each patch meeting the minimum size constraint, the average Euclidean distance (y) along the perimeter was found for actual distances (x) of 4, 8, **16,** 32, 64, 128, and 512 cells. The portions of patch perimeters that touched the map border were excluded.

PENT: Fractal estimator of patch configurational entropy from the scaling of patch density to the size of a neighborhood of an arbitrary cell in the patch (Vos 1988).

Let $Z_f(L)$ be the probability, for an arbitrary cell in a patch, of findingfother cells of the same patch within a square of side length L centered on the arbitrary cell. For example, $Z_2(5)$ is the probability of finding two more cells of a patch in a **5** x 5 square centered on an arbitrary cell in the patch. In general,

$$Z_f(L) = \frac{S_{f,L}}{S_k^*}$$

where the numerator is the number of cells for which **f** was realized for length L, and the denominator is the number of cells sampled.

Let $N(L)$ be the maximum number of cells of the same patch observed in any square of size L Define

---

[5] Riitters, K.H. Fractal dimensions from partial perimters. Unpublished manuscript.

$$M^0(L) = \Sigma_{f=1}^{N(L)} \ln(f)\, Z_f(L)$$

From each patch with size > 400 cells, a random sample of at least 400 cells was selected. Square neighborhoods of size L = 5, 15, 25, 35, and 45 were placed around each sample cell, and the occurrences of cells of the same patch were counted for each neighborhood size. The values of $Z_f(L)$ and $M^0(L)$ were calculated after the counts are accumulated for all sampled cells. Let β_{7v} be the estimated slope from the regression of $M^0(L)$ on $\ln(L)$ for the v-th patch. The fractal estimator is given by:

$$PENT = \frac{1}{u} \Sigma_{v=1}^{u} \beta_{7v}$$

PMAS: Fractal estimator of patch mass from the scaling of patch density to the size of a neighborhood of an arbitrary cell in the patch (Voss 1988).

Define

$$M^1(L) = \Sigma_{f=1}^{N(L)} f\, Z_f(L)$$

Let β_{8v} be the estimated slope from the regression of $\ln(M^1(L)$ for the v-th patch. The fractal estimator is:

$$PMAS = \frac{1}{u} \Sigma_{v=1}^{u} \beta_{8v}$$

PVAR: Fractal estimator of patch variance from the scaling of patch density to the size of a neighborhood of an arbitrary cell in the patch (Voss 1988).

Define

$$M^2(L) = \Sigma_{f=1}^{N(L)} f^2\, Z_f(L)$$

Let β_{9v} be the estimated slope from the regression of $\ln(M^2(L))$ on $\ln(L)$ for the v-th patch. The fractal estimator is:

$$PVAR = \frac{1}{u} \Sigma_{v=1}^{u} \beta_{9v}$$

PLAC: Average large-patch lacunarity. (Note: this simple estimator of lacunarity is approximate at best, and it is different from the estimator described by Plotnik *et al.* [1993]).

$$\mathrm{PLAC} = \mathrm{PVAR} - \mathrm{PENT}$$

TENT: Average fractal estimator of attribute class configurational entropy from the scaling of attribute class density to the size of a neighborhood of an arbitrary cell in the class.

This development follows that presented for PENT, except the metric applies to attribute classes rather than to patches. Let $Q_f(L)$ be the probability, for an arbitrary cell in an attribute class, of finding f other cells of the same class within a square of side length L centered on the arbitrary cell. In general,

$$Q_f(L) = \frac{s_{f,L}}{F_i}$$

where the numerator is the number of cells for which **f** was realized for length L, and the denominator is the number od cells sampled.

Let $N(L)$ be the maximum number of cells of the same class observed in any square of size L. Define

$$M^0(L) = \Sigma_{f=1}^{N(L)} \ln(f)\, Q_f(L)$$

From each attribute class with > 400 cells, a random sample of at least 400 cells was selected. Square neighborhoods of size L = 5, 15, 25, 35, and 45 were placed around each sampled cell, and the occurrence of cells of the same class were counted for each neighborhood size. The values of $Q_f(L)$ and $M^0(L)$ were calculated after the counts are accumulated for all sampled cells. Let β_{10i} be the estimated slope from the regression of $M^0(L)$ on $\ln(L)$ for the i-th attribute class. The fractal estimator is:

$$\mathrm{TENT} = \Sigma_{i=1}^{t} w_i\, \beta_{10i}$$

TMAS: Fractal estimator of attribute class mass from the scaling of attribute class density to the size of a neighborhood of an arbitrary cell in the class.

Define

$$M^1(L) = \Sigma_{f=1}^{N(L)} f\, Q_f(L)$$

Let β_{11i} be the estimated slope from the regression of $\ln(M^1(L))$ on $\ln(L)$ for the i-th attribute class. The fractal estimator is:

$$\mathrm{TMAS} = \Sigma_{i=1}^{t} w_i\, \beta_{11i}$$

TVAR: Fractal estimator of attribute class variance

from the scaling of attribute class density to the size of a neighborhood of an arbitrary cell in the class.

Define

$$M^2(L) = \Sigma^{N(L)}_{f=1} f^2 Q_f(L)$$

Let β_{12i} be the estimated slope from the regression of $\ln(M^2(L))$ on $\ln(L)$ for the i-th attribute class.

The fractal estimator is:

$$TVAR = \Sigma^{t}_{i=1} w_i \beta_{12i}$$

TLAC: Average attribute class lacunarity.

$$TLAC = TVAR - TENT$$